Open access • Journal Article • DOI:10.1097/PAS.0B013E31824A7B1A

The clinicopathologic features of YWHAE-FAM22 endometrial stromal sarcomas: a histologically high-grade and clinically aggressive tumor. — Source link

Cheng-Han Lee, Adrián Mariño-Enríquez, Wen-Bin Ou, Meijun Zhu ...+10 more authors

Institutions: Brigham and Women's Hospital

Published on: 01 May 2012 - The American Journal of Surgical Pathology (Am J Surg Pathol)

Topics: Endometrial stromal sarcoma and YWHAE

The Clinicopathologic Features of *YWHAE-FAM22* Endometrial Stromal Sarcomas: A Histologically High-grade and Clinically Aggressive Tumor

Cheng-Han Lee, MD, PhD,† Adrian Mariño-Enriquez, MD,* Wenbin Ou, PhD,* Meijun Zhu, PhD,* Rola H. Ali, MD,† Sarah Chiang, MD,‡ Frédéric Amant, MD,§ C. Blake Gilks, MD,† Matt van de Rijn, MD, PhD,‖ Esther Oliva, MD,‡ Maria Debiec-Rychter, MD,¶ Paola Dal Cin, PhD,* Jonathan A. Fletcher, MD,* and Marisa R. Nucci, MD**

Abstract: Endometrial stromal sarcoma (ESS) is a genetically heterogenous group of uterine sarcomas, of which almost half are associated with *JAZF1* rearrangement. We recently identified a novel genetic fusion between *YWHAE* and *FAM22A/B* in ESS harboring t(10;17)(q22;p13) and herein describe the clinicopathologic features of 13 *YWHAE-FAM22* ESS cases (11 primary and 3 metastatic) and compare them with 20 ESS cases with *JAZF1* rearrangement. Ten of 11 primary uterine tumors contained morphologically high-grade areas composed of round cells arranged in nests with a delicate stromal capillary network. The tumor cells showed large nuclei with irregular nuclear contours and significant mitotic activity (> 10 mitoses/10 HPF) in addition to focal tumor necrosis, in contrast to *JAZF1* ESS, which lacked a nested growth pattern, were composed of cells with small round/oval nuclei, and typically had < 5 MF/10 HPF. In 7 of the 11 uterine tumors, there was an additional cytologically bland and mitotically weakly active spindle cell component with a fibrous/fibromyxoid stroma (ESS, fibromyxoid variant). Two metastatic tumors (pulmonary) also contained round cell and spindle cell components, whereas 1 metastasis (vaginal) was composed solely of the spindle cell component. In both primary and metastatic tumors, the spindle cells were diffusely positive for estrogen and progesterone receptors and CD10, in contrast to the round cell areas, which were negative. Clinically, 10 of 12 patients with *YWHAE-FAM22* ESS presented with FIGO stages II to III disease, in contrast to only 4 of 16 patients with *JAZF1* ESS presenting with stages II to III disease ($P < 0.05$). Tumors with *YWHAE-FAM22* rearrangements constitute a distinct group of ESS, which is associated with high-grade morphology and aggressive clinical behavior compared to *JAZF1* ESS. Thus, their distinction from typical *JAZF1* ESS is important for prognostic and therapeutic purposes.

Key Words: endometrial stromal sarcoma, 14-3-3, *YWHAE*, *FAM22*, *JAZF1*

(*Am J Surg Pathol* 2012;00:000–000)

From the *Department of Pathology, Brigham and Women's Hospital; ‡Department of Pathology, Massachusetts General Hospital, Boston, MA; †Department of Pathology, Vancouver General Hospital, Vancouver, BC, Canada; Departments of §Oncology; ¶Human Genetics, Catholic University Leuven and University Hospital, Leuven, Belgium; and ‖Department of Pathology, Stanford University Medical Center, Stanford, CA.

Presented in a platform presentation at USCAP 2011 annual meeting (San Antonio, USA)—abstract 1081 published in *Modern Pathology*, 2011;24(S1):255A.

A.M.-E. is supported by a research grant from Fundación Alfonso Martín Escudero, Madrid, Spain.

Conflicts of Interest and Source of Funding: The authors have disclosed that they have no significant relationships with, or financial interest in, any commercial companies pertaining to this article.

Correspondence: Marisa R. Nucci, MD, Department of Pathology, Brigham and Women's Hospital, 75 Francis Street, Amory 3, Boston, MA 02115 (e-mail: mnucci@partners.org).

Supplemental digital content is available for this article. Direct URL citations appear in the printed text and are provided in the HTML and PDF versions of this article on the journal's Website, www.ajsp.com.

Endometrial stromal sarcoma (ESS) is the second most common malignant uterine mesenchymal tumor, and it affects women primarily in the perimenopausal age group. These tumors are composed of cells that morphologically resemble non-neoplastic proliferative-phase endometrial stroma and have been termed "low-grade ESS" according to the current WHO classification to reflect their highly differentiated state. Classically, the tumor cells have bland nuclear features with monotonous oval to spindle cells concentrically proliferating around a rich vascular network of arterioles and capillaries; mitotic activity is typically low (< 5 per 10 HPF), and tumor necrosis is absent in most tumors.[8,9,31] The WHO also recognizes another category of malignant stromal neoplasia, termed undifferentiated endometrial sarcoma (UES). In contrast to low-grade ESS, UES by definition does not resemble endometrial stroma; instead, it exhibits high-grade cytologic atypia with marked nuclear pleomorphism accompanied in most instances by a high mitotic rate and the presence of tumor necrosis. Distinction between ESS and UES is crucial because of major differences in prognosis between these 2 tumor types (5 y survival approximately

85% in ESS vs. < 50% in UES patients).[8,2,5,7,11–13] In recent years it has become increasingly clear that this binary classification scheme does not adequately reflect the morphologic diversity that can occur in malignant stromal tumors. For example, some uterine sarcomas can display cytologic and immunohistochemical features that are intermediate between classic low-grade ESS and UES, which has been described in the literature as UES with nuclear uniformity.[20] Moreover, other tumors may show areas of UES juxtaposed to low-grade areas. In both instances, however, tumors behave in a more aggressive manner compared with classic low-grade ESS. In addition to high-grade cytologic features, ESS can also display variant histologic appearances, including smooth muscle, sex cord, glandular, and fibrous differentiation.[31]

In keeping with the varied histologic appearance, ESS as currently defined is genetically heterogenous as well.[38] Even though approximately 50% to 60% of ESS cases demonstrate a rearrangement of genes involved in chromatin binding (*JAZF1*, *SUZ12*, *PHF1*, *EPC1*), most commonly in the form of t(7;17)(p15;q21), which results in *JAZF1-SUZ12* genetic fusion,[20,10,15,16,19,27,28,32] little is known about the genetics of the remaining tumors. ESS harboring t(7;17) and *JAZF1-SUZ12* genetic fusion tends to display a classic low-grade morphology, including variants.[16] Although rare cases of ESS harboring *JAZF1* rearrangement can show higher-grade histologic features at initial presentation,[20] these tend to be observed in recurrent tumors,[4,30] and the genetics of a significant subset of ESS, especially ones with higher-grade histologic features, remain undefined.

We recently identified the genes rearranged in t(10;17)(q22;p13), a recurrent aberration previously reported in ESS[3,24,28,37] and in a subset of clear cell sarcoma of the kidney,[6,35,36] and the rearrangement results in an in-frame fusion between *YWHAE* (exons 1 to 5) and 1 of the 2 highly homologous genes *FAM22A* and *FAM22B* (exons 2 to 7) (designated as *YWHAE-FAM22*).[23] The goal of this study is to report the clinical and histopathologic features of primary and metastatic ESS associated with *YWHAE-FAM22* rearrangements.

METHODS

Tumor Samples

Formalin-fixed paraffin-embedded tumor tissues from 13 ESS with *YWHAE-FAM22* rearrangement and 20 molecularly confirmed *JAZF1*-rearranged ESS were obtained from the pathology archives at Brigham and Women's Hospital (BWH), Catholic University of Leuven (KUL), Massachusetts General Hospital (MGH), and Vancouver General Hospital (VGH). The histologic features of all tumors were reviewed by 2 authors (C.H.L. and M.R.N.). The study has been approved by the respective Institutional Review Boards.

Fluorescence In Situ Hybridization (FISH)

FISH probes flanking genes of interest (*YWHAE*, *FAM22A*, and *FAM22B*) shown in supplemental Figure 1, Supplemental Digital Content 1, http://links.lww.com/PAS/A112, were prepared from BAC clones (CHORI). FISH was performed on 4-μm-thick full sections and tissue microarray sections using a standard pretreatment and hybridization protocol.[25] The slides were reviewed manually with at least 50 tumor nuclei evaluated for each case, and a cutoff of > 30% nuclei showing a split signal was used to be considered positive for rearrangement of the flanked gene (supplemental Figure 1, Supplemental Digital Content 1, http://links.lww.com/PAS/A112). Normal paired signals are defined as an orange and green signal less than 3 signal diameters apart or as a single yellow (overlapping) signal, whereas unpaired signals are those separated by ≥ 3 signal diameters. For tissue microarray sections, all cores with complete or partial loss of tumor tissue (< 50 tumor nuclei) or with weak signals were excluded from the analysis. To be considered positive for *YWHAE-FAM22A/B* rearrangement, an individual case needs to demonstrate concomitant rearrangement in *YWHAE* and *FAM22A* or in *YWHAE* and *FAM22B* by FISH analysis.

Immunohistochemistry

Immunohistochemical analysis was performed on whole sections of the 11 primary *YWHAE-FAM22* ESS and 2 metastatic *YWHAE-FAM22* ESS cases. Estrogen receptor (ER, Thermo Fisher, SP1, 1:60 dilution, citrate buffer pressure cook), progesterone receptor (PR, Dako, PGR636, 1:200 dilution, citrate buffer pressure cook), and CD10 (Vector lab, 56C6, 1:10 dilution, citrate buffer pressure cook) immunostaining was performed according to the manufacturer's recommendations using the EnVision+ System-HRP (Dako) on an automated instrument (Dako Autostainer Plus, Dako). For Ki-67 (Labvision, clone SP6, 1:200 dilution), antigen retrieval was performed using CC1 antigen retrieval buffer (Ventana Medical Systems, AZ). For ER and PR, moderate to strong nuclear staining in > 5% of tumor cells was considered positive. For CD10, moderate to strong cytoplasmic staining in > 30% of tumor cells was considered positive. Ki-67 staining was evaluated manually on the basis of assessment of 100 tumor cell nuclei in representative areas.

RESULTS

Clinical Features of ESS With YWHAE-FAM22 and Comparison with JAZF1-rearranged ESS

A total of 13 primary and/or metastatic uterine sarcomas were found to harbor *YWHAE* and *FAM22A/B* genetic rearrangement by FISH analysis (Table 1 and supplemental Figure 1, Supplemental Digital Content 1, http://links.lww.com/PAS/A112). The 13 patients ranged in age from 28 to 67 (mean 50) years at the time of initial diagnosis (Table 1). The most common presenting symptom for patients with uterine *YWHAE-FAM22* ESS was abnormal vaginal bleeding (menorrhagia or peri/postmenopausal bleeding). Staging information was available for 12 of 13 patients (Table 1). By the most recent FIGO staging criteria (2009), 10 of 12 (83%) patients presented with stages II to III disease (stages III to

TABLE 1. Clinical Features of *YWHAE-FAM22* ESS

Case	Source	Age at Diagnosis	Clinical Presentation	Karyotype	FISH Result	FIGO Stage (2009)	Follow-up
1	BWH	47	Menorrhagia	46, XX, t(10;17)(q22;p13)	*YWHAE-FAM22B*	Stage I	AWD (5 y; progressive disease with pulmonary recurrence)
2	BWH	67	Vaginal bleeding	44, XX, der(5)t(5;21)(q35;q11), der(11)t(9;11)(q10;q10), −10, t(10;17)(q22;p13), −21	*YWHAE-FAM22A*	Stage IB	AWD (1.5 y; progressive abdominal recurrence)
3	BWH	45	Vaginal bleeding	44, XX, t(10;17)(q22;p13), del(11)(q1?2), −19, −22	*YWHAE-FAM22A*	Stage IIIB	NED (3.75 y)
4	BWH	43	NA	45, X, -X, t(10;17;12) (q22; p11.2;q13), add(19) (p13.3)	*YWHAE-FAM22B*	NA	Alive (disease status unknown)
5	VGH	57	NA	NA	*YWHAE-FAM22B*	Stage IIIC	DOD (2 y)
6	BWH	62	Vaginal bleeding	NA	*YWHAE-FAM22B*	Stage IIB	AWD (1 y)
7	BWH	54	Vaginal bleeding	NA	*YWHAE-FAM22B*	Stage IIA	AWD (1 y; progressive disease with abdominal and pulmonary recurrence)
8	BWH	49	Abdominal mass	NA	*YWHAE-FAM22B*	Stage IIIC	DOD (2 y)
9	KUL	28	NA	46, XX, t(10;17)(q22;p13)	*YWHAE-FAM22B*	Stage IIB	AWD (9 y)
10	KUL	50	NA	47, XX, t(10;17)(q22;p13.3),- −11, + 19, + mar[20].	*YWHAE-FAM22B*	Stage IIIC	AWD (1 y)
11	KUL	66	NA	46, XX, t(4;10;17)(q12;q22;p13)	*YWHAE-FAM22B*	Stage IIB	AWD (10 y)
12	BWH	49	Menorrhagia	46, XX, t(10;17)(q22;p13)	*YWHAE-FAM22B*	Stage IIB	NA
13	MGH	56	NA	46, XX, t(10;17)(q22;p13)	*YWHAE-FAM22B*	Stage IIB	NA

AWD indicates alive with disease; DOD, died of disease; NA, not available; NED, alive with no evidence of disease.

IV disease by the former FIGO stating criteria), where there is evidence of extrauterine tumor extension. Of the 2 patients with FIGO stage I tumors at presentation, 1 developed pulmonary metastases a year later, and she is alive with disease 5 years after the initial diagnosis, whereas the other patient developed multiple peritoneal recurrences a year later and is alive with disease 1.5 years after the initial diagnosis.

Clinical follow-up (at least 1 y with an average of 3.5 y) information was available for 10 patients (Table 1). Two died from progressive disease 2 years later, and 7 patients were alive with disease (ranging from 1 to 10 y) after the initial diagnosis. The latter had a combination of pelvic/peritoneal and/or distant recurrence (pulmonary metastases in 4 patients). Only 1 patient had no evidence of disease with a follow-up of 3.75 years; she originally presented with stage IIIB ESS and underwent total abdominal hysterectomy and bilateral salpingo-oophorectomy with pelvic/peritoneal tumor debulking followed by 5 cycles of chemotherapy (adriamycin and ifosfamide with mesna support). All of the patients were treated surgically with total hysterectomy and adnexectomy (+/− pelvic/peritoneal tumor debulking) for the primary disease.

Staging data were available for 16 of 20 patients with *JAZF1*-rearranged ESS, and only 4 of 16 (25%) had FIGO 2009 stages II to III disease (stages III to IV disease by former FIGO staging criteria). Follow-up information was available for 17 of 20 patients with *JAZF1*-rearranged ESS. Among these 17 patients, 13 (76%) were alive and well (follow-up period ranging from 1 to 34 y, average 10 y), 2 were alive with disease, whereas 2 died of the disease (within a month and 9 y after the initial diagnosis, respectively).

Histopathologic Features of ESS Harboring YWHAE-FAM22 Genetic Fusion and Comparison with JAZF1-rearranged ESS

The primary site for all 13 *YWHAE-FAM22* ESS cases was the uterine corpus (Fig. 1). The uterine tumors ranged in size from 3 to 9 (median 7.5) cm (Table 2). It is

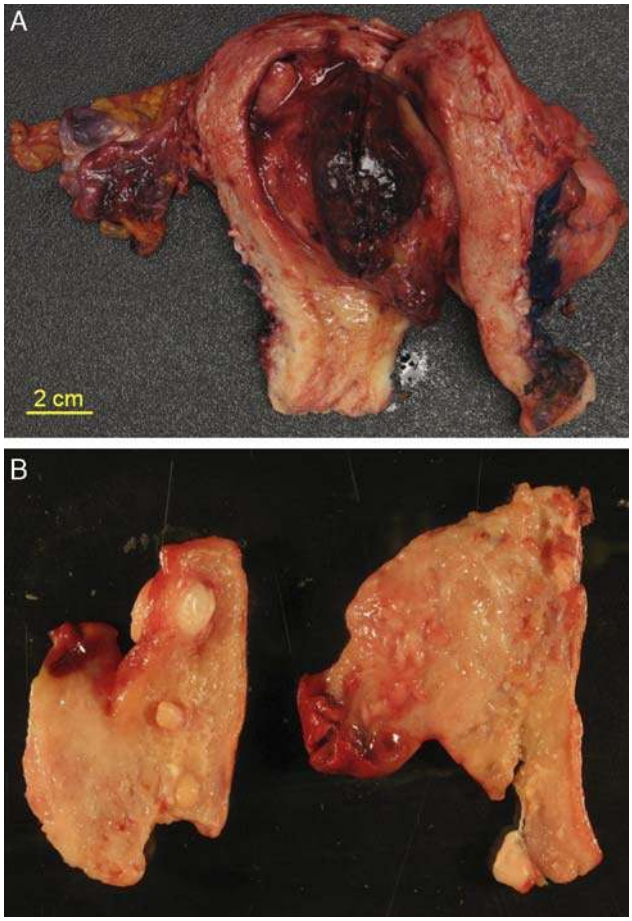

FIGURE 1. Gross images of a *YWHAE-FAM22* ESS (case number 12, Table 1) forming a large mass (9 cm) in the posterior uterine wall (A) bivalved uterus, (B) cross-sections of the posterior uterine wall).

noteworthy that 1 ESS with bulky retroperitoneal tumor (measuring approximately 27 cm) showed a 1 cm tumor in the endometrial cavity. In 11 of 13 cases, the primary tumor was available for histologic review (1 with both primary and pulmonary metastases), whereas only metastatic tumor was available for review in the 2 remaining cases. Within the uterus, all *YWHAE-FAM22* ESS cases showed extensive permeative growth through the myometrium (similar to that seen in *JAZF1*-rearranged ESS), with invasion well into the outer half of the myometrium (Figs. 2A, B). Vascular invasion was present in all cases.

Of the 11 primary uterine tumors, 7 contained a mixture of round cell and spindle cell areas, whereas 3 and 1 showed a purely round cell and purely spindle cell appearance, respectively (Table 2). *YWHAE-FAM22* genetic rearrangement was demonstrated by FISH in both the round cell and spindle cell areas in tumors showing a mixture of the 2 components. The round cell component was highly cellular, and the tumor cells were typically arranged in a vaguely nested growth pattern (Figs. 2C–F), with the nests being separated by a delicate stromal capillary network. These cohesive round cells had scanty (small round blue cell appearance; Figs. 2D, F) to moderate eosinophilic (epithelioid appearance) cytoplasm (Figs. 2C, E). The round cell component showed no significant pleomorphism in nuclear size on low-power ($\times 4$ objective) assessment. On high-power examination, the round cells contained nuclei that were 4 to 6 times the size of background lymphocyte nuclei (Figs. 3A, B). More importantly, the nuclei exhibited an irregular membrane with angulated contour. In contrast, the nuclei of *JAZF1*-rearranged ESS were generally smaller in size (2 to 4 times the size of background lymphocyte nuclei), and all displayed a smooth nuclear contour (Figs. 3C, D). The chromatin was finely granular to slightly vesicular in appearance without prominent nucleoli. In a subset of tumors the cells were less cohesive, displaying a pseudoglandular or pseudopapillary architecture (Fig. 4A). Focal sex-cord–like differentiation was present in the round cell area of 2 tumors (Fig. 4B). A high mitotic rate ($>$ 10/10 HPF, up to 77/10 HPF) was seen in 10 of 11 primary uterine and 2 of 3 metastatic tumors; no atypical mitotic figures were identified. Tumor necrosis was present in 10 of 11 primary tumors, and it ranged from multifocal patchy necrosis to extensive geographic necrosis. Mitotic rate in 11 *JAZF1*-rearranged ESS cases ranged from 1 to 8 MF/10 HPF with an average of 3 MF/10 HPF; only 2 showed $>$ 5 MF/10 HPF. Focal tumor necrosis was seen in 5 cases. The difference in the histologic appearance of *YWHAE-FAM22* ESS and *JAZF1*-rearranged ESS has been summarized in Table 3.

The spindle cell component was closely juxtaposed to the round cell component in the 7 cases with mixed round and spindle cell areas (Figs. 4C, D). It showed low to intermediate cellularity and consisted of a proliferation of monomorphic cytologically bland spindle cells embedded in a fibrocollagenous to fibromyxoid matrix (Figs. 4E, F). The nuclei were ovoid to oblong in shape but had more pointed ends (in comparison with myometrial smooth muscle cells), and the chromatin was finely dispersed with no discernible nucleoli. These spindle cells were arranged in loose fascicles in most instances but formed intersecting fascicles closely mimicking a smooth muscle tumor in 2 tumors (smooth muscle actin and desmin negative) (Figs. 4G, H). Mitotic activity was low ($\leq$ 3 MF/10 HPF).

In the one ESS in which both the primary uterine tumor and the subsequent pulmonary metastasis were available for review (both demonstrating the *YWHAE* rearrangement), the uterine tumor that was removed in a piece-meal manner in a supracervical hysterectomy showed spindle morphology with low-grade nuclear features, low mitotic rate (3 MF/10 HPF), and no tumor necrosis. The pulmonary metastasis that developed a year later showed mixed high-grade round cell and low-grade spindle cell components, with the spindle cell area encircling the round cell area. The round cell component consists of cohesive nests of tumor cells with either scanty or moderate amounts of cytoplasm and focally discohesive pseudopapillary areas. In contrast to the uterine

TABLE 2. Histologic and Immunohistochemical Features of *YWHAE-FAM22* ESS

Case	Tumor Examined	Size (cm)	Original Diagnosis	Cell Morphology	Nuclear Grade	Mitosis (10 HPF)	Necrosis	Immunophenotype
1	Uterine primary	NA	Low-grade ESS	Spindle cell (fibrous)	LG	3	Absent	$CD10^+$
	Metastasis to lung		ESS, histologically high grade	Round cell and spindle cell (fibrous)	HG	56	Focal	$ER/PR/CD10^+$ in spindle cell area only
2	Uterine primary	8.5	Uterine sarcoma, intermediate to high grade	Round cell and spindle cell (fibrous)	HG	27	Focal	$ER/PR/CD10^+$ in spindle cell area only
3	Uterine primary	3.1	Poorly differentiated uterine sarcoma	Round cell and spindle cell (fibromyxoid)	HG	20	Focal	$ER/PR/CD10^+$ in spindle cell area only
4	Metastasis to lung	NA	High-grade round cell neoplasm	Round cell	HG	19	Focal	NA
5	Uterine primary	8	UES	Round cell	HG	15	Focal	$ER/PR/CD10^-$
6	Uterine primary	8.8	ESS, morphologically high grade	Round cell and spindle cell (fibromyxoid)	HG	18	Focal	$ER/PR/CD10^+$ in spindle cell area only
7	Uterine primary	7.2	High-grade ESS	Round cell and spindle cell (fibrous)	HG	25	Extensive	$ER/PR/CD10^+$ in spindle cell area only
8	Uterine primary	12	ESS with high-grade areas	Round cell and spindle cell (fibrous)	HG	21	Focal	$ER/PR/CD10^+$ in spindle cell area only
9	Uterine primary	7.5	ESS vs. UES	Round cell	HG	20	Focal	$ER/PR/CD10^-$
10	Uterine primary	4.2	UES	Round cell	HG	29	Focal	$ER/PR/CD10^-$
11	Metastasis to vaginal wall	1.5	ESS	Spindle cell (fibrous)	LG	1	Absent	$ER/PR/CD10^+$
12	Uterine primary	9	High-grade ESS	Round cell and spindle cell (fibrous)	HG	15	Focal	$ER/PR/CD10^+$ in spindle cell area only
13	Uterine primary	1*	ESS, histologically high grade	Round cell and spindle cells (fibrous)	HG	77	Extensive	$ER/PR/CD10^+$ in spindle cell area only

*1 cm tumor in the endometrial cavity with 27 cm extrauterine mass.
HG indicates high grade; LG, low grade; NA, not available.

primary, the round cell component of the metastatic tumor demonstrated considerably higher mitotic rate (up to 58 MF/10 HPF).

In 2 additional cases, only metastatic tumor was available for review, corresponding to vaginal and pulmonary metastasis, respectively. In the first case, the tumor in the vagina was composed of spindle cells with a small amount of pale cytoplasm, low-grade nuclear features, and infrequent mitoses (1/10 HPF). The pulmonary metastasis consisted of purely high-grade round cells with focal rhabdoid features and displayed a high mitotic (19 MF/10 HPF) rate with focal tumor necrosis.

Immunophenotypic Features of YWHAE-FAM22 ESS

The immunoprofile of the 13 *YWHAE-FAM22* ESS cases is summarized in Table 2. Of the 11 uterine tumors, tumor cells in the round cell component were all CD10 negative; 3 were also ER and PR negative. Minimal (< 5%) weak to moderate ER or PR staining within the round cell areas was seen in 7 tumors, particularly in cells of perivascular location. In contrast, the spindle cell component in all tumors was always diffusely and strongly CD10, ER, and PR positive (Figs. 4H, 5A–C). There was no difference in the patterns of staining for CD10, ER, and PR between the primary and metastatic tumors. Ki-67 proliferation index was examined in 4 *YWHAE-FAM22* ESS cases (cases 1, 2, 3, and 5), and the round cell component showed 24%, 16%, 28%, and 32% proliferation indices, respectively (Fig. 5D). The spindle cell component present showed < 1% Ki-67 proliferation index. In addition, on the basis of the panel of immunomarkers used for staining by the original sign-out pathologists, the round cell component, including the pseudoglandular and pseudopapillary foci, was consistently negative for epithelial (4), smooth muscle (8), or melanocytic markers (3). The spindle cell component (including areas closely mimicking smooth muscle) was negative for smooth muscle actin, desmin, and caldesmon (5). ER, PR, CD10, and Ki-67 staining was evaluated in 10 *JAZF1*-rearranged ESS cases with available material. ER was positive in 9 of 10, PR in 8 of 10, and CD10 in 7 of 10 cases, with the staining being usually diffuse and strong in the positive cases. Ki-67 labeling index ranged from < 1% to 8% (average of 3%) (Fig. 5E).

Karyotypes of YWHAE-FAM22 ESS

Cytogenetic analysis was performed on 9 of the 13 *YWHAE-FAM22* ESS, and the results are summarized in Table 1. All 9 cases displayed t(10;17)(q22;p13) as the main cytogenetic aberration (Fig. 6).

DISCUSSION

ESS is currently defined as a neoplasm composed of cells resembling proliferative-phase endometrial stroma that infiltrates the surrounding myometrium in a characteristic "finger-like" permeative manner and typically invades lymphatic or vascular spaces.[14] Implicit in the current WHO definition is the requirement that ESS demonstrate a "highly differentiated" (ie, close resemblance

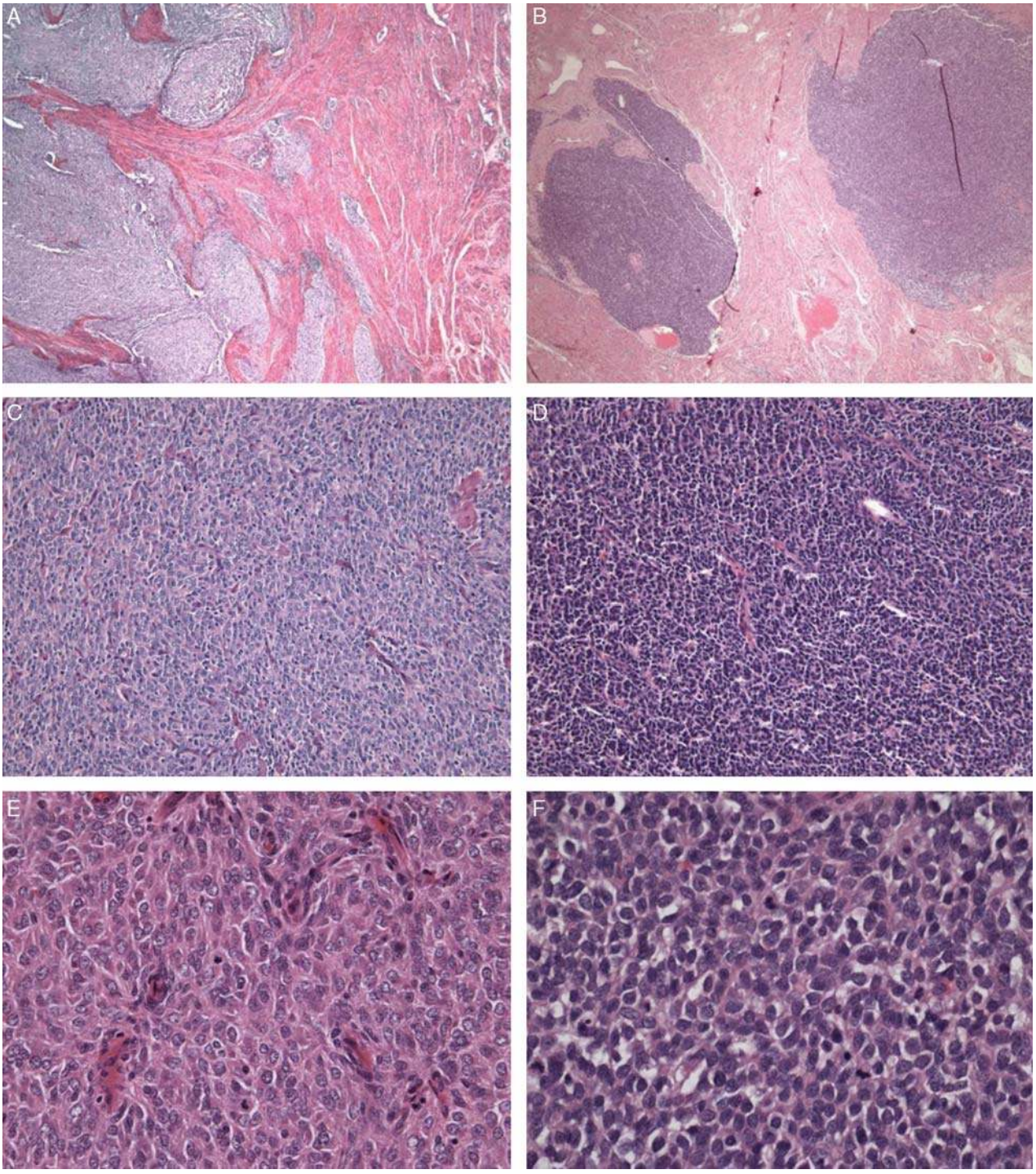

FIGURE 2. Representative images showing the high-grade round cell component of *YWHAE-FAM22* ESS at different magnifications. The tumor shows extensive permeative growth through the myometrium (A and B). The amount of cytoplasm in tumor cells can be moderate (C and E) to scanty (D and F).

to non-neoplastic endometrial stroma) morphologic appearance. In the past, tumors that had the appearance of proliferative-phase endometrial stroma but had mitotic activity that exceeded 10 mitoses/10 HPF were classified as "high-grade ESS"; however, as normal endometrial stroma can exhibit significant mitotic activity, particularly in its proliferative phase, it is currently accepted that classic "low-grade" ESS should not be classified as "high-grade" on the basis of mitotic activity alone.[8] Therefore, the current WHO classification scheme recognizes 2

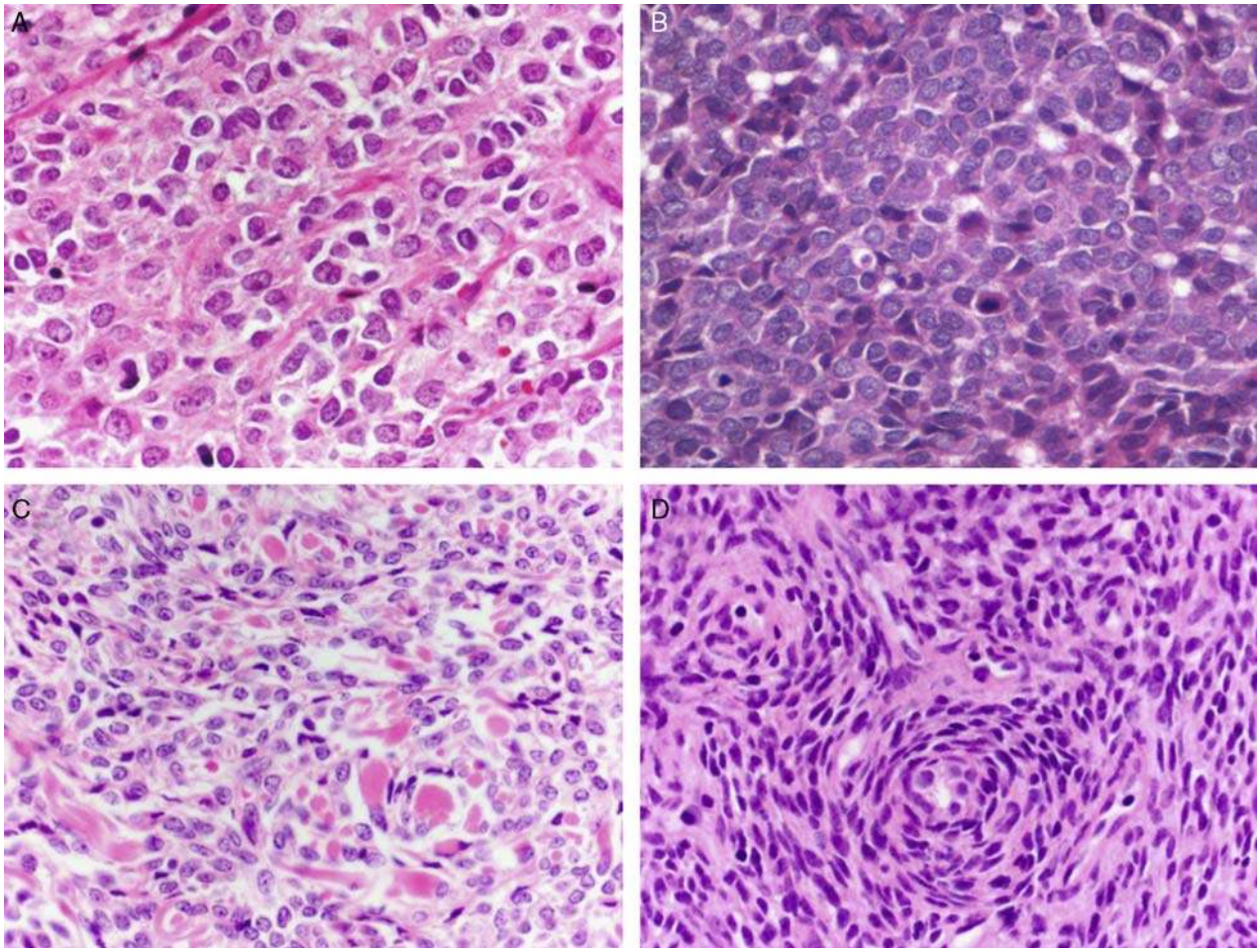

FIGURE 3. Representative high-power images comparing the round cell component in 2 different *YWHAE-FAM22* ESS cases (A and B) with 2 different *JAZF1*-rearranged ESS cases (C and D). All images were taken at the same magnification. The round cell component of *YWHAE-FAM22* ESS displays higher-grade nuclear features compared with *JAZF1*-rearranged ESS, with larger nuclear size and more irregular nuclear contour.

categories of endometrial sarcoma—low grade and undifferentiated—which are based on differences in tumor morphology rather than on mitotic activity. A UES, as currently defined, is a poorly differentiated sarcoma composed of cells that do not resemble proliferative-phase endometrial stroma but is composed of larger cells with high-grade nuclear atypia. In addition, these tumors typically show destructive but not permeative infiltration of the myometrium. Despite this attempt to separate these tumors into binary low-grade and high-grade diagnostic categories, there are examples of endometrial sarcoma that have features of both UES and low-grade ESS. These tumors display either (1) a combination of low-grade and undifferentiated areas; (2) cytologic and immunohistochemical features that are intermediate between classic low-grade ESS and UES; or (3) cytologic features of UES but with the presence of finger-like infiltrative pattern of the surrounding myometrium or extension into lymphatic or vascular spaces typical of its low-grade counterpart.

As illustrated in our series, although both *YWHAE-FAM22* ESS and *JAZF1*-rearrarranged ESS show a similar infiltrative pattern through the uterine wall, the former typically exhibits histologically distinctive features that allow its recognition and separation from the latter. In fact, most tumors were diagnosed by the original diagnostician as UES or high-grade uterine sarcoma, and in cases in which the diagnosis of ESS was rendered they were usually additionally qualified as high-grade ESS or ESS with high-grade areas/features. In the single case in which sections of the primary uterine tumor showed only low-grade spindle/ovoid cell morphology in a fibrous matrix, the patient developed pulmonary metastasis a year later, and the metastatic tumor exhibited admixed high-grade round cell and low-grade spindle cell areas. As the uterine tumor was removed in a piece-meal manner in a supracervical hysterectomy procedure with 7 representative sections submitted, it is plausible that a high-grade round cell component was present but not sampled in the hysterectomy specimen, particularly as all

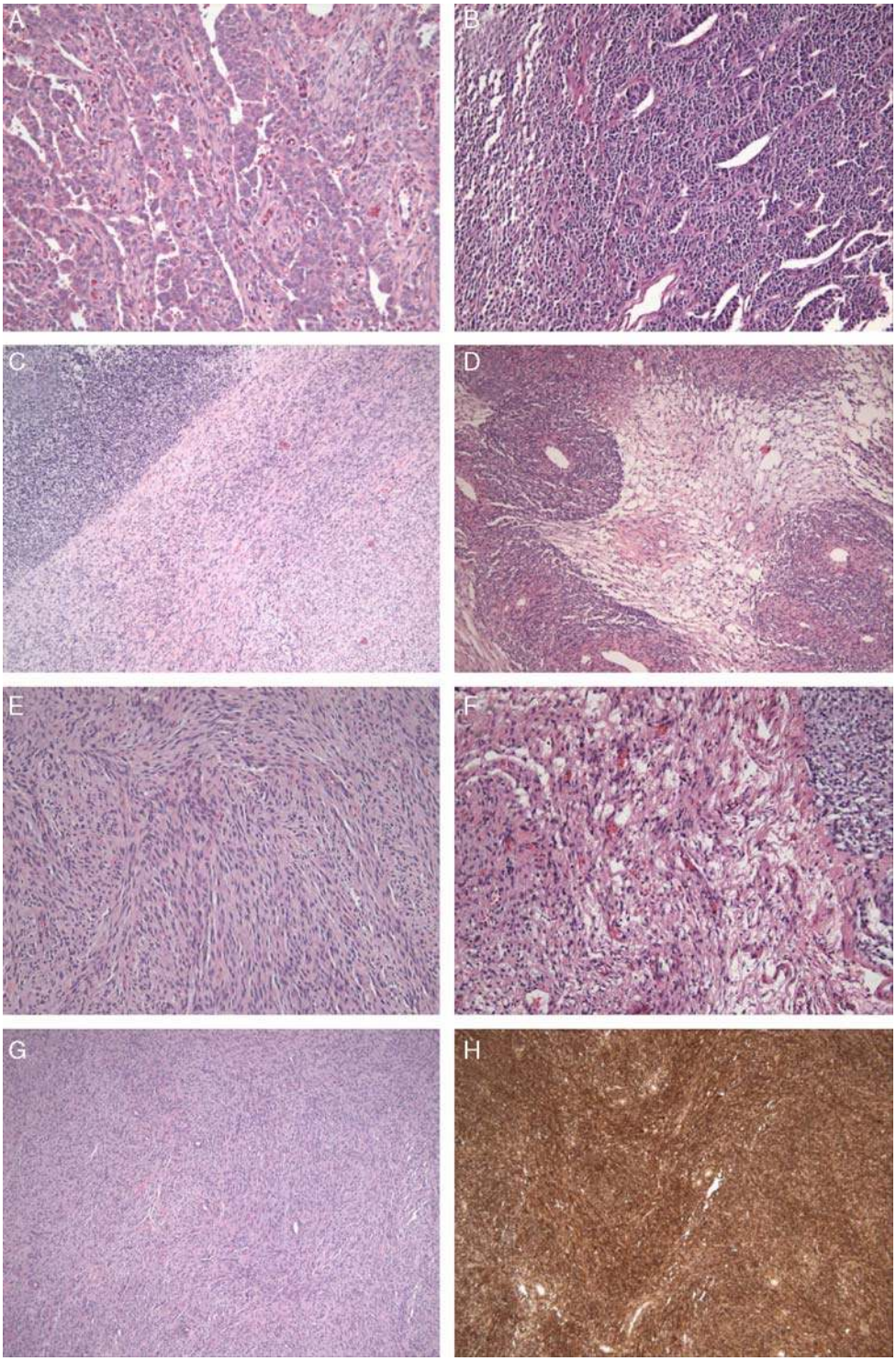

FIGURE 4. Variant morphologic features of *YWHAE-FAM22* ESS. Occasional *YWHAE-FAM22* ESS can show pseudoglandular/pseudopapillary pattern (A) or focal sex-cord–like differentiation (B). A significant subset of *YWHAE-FAM22* ESS displays a biphasic appearance with mixed high-grade round cell and low-grade spindle cell components (C and D). The spindle cell component shows moderate cellularity with a fascicular growth pattern, and the stroma can be fibrous (E) to fibromyxoid (F). The spindle cell component (G) demonstrates diffuse CD10 immunoreactivity (H).

TABLE 3. Morphologic Comparison Between *JAZF1*-rearranged ESS and *YWHAE-FAM22* ESS

	JAZF1-rearranged ESS	*YWHAE-FAM22* ESS	
Growth Features			
Myopermeative growth	Present	Present	
Vascular invasion	Frequent	Frequent	
Biphasic appearance*	Rare	Frequent	
Stromal vasculature	Prominent arterioles with periarteriolar whorling of tumor cells	Prominent thin-wall capillary network in the round cell component	
Cytologic Features		**Round Cell Component**	**Spindle Cell Component**
Nuclear shape	Round to fusiform	Round	Fusiform to spindle
Nuclear size	Small (2–4× of lymphocyte nuclei)	Large (4–6× of lymphocyte nuclei)	Similar to the size of normal smooth muscle nuclei
Nuclear membrane	Very smooth contour	Irregular contour	Smooth contour
Nuclear pleomorphism	Nonpleomorphic (very uniform)	Nonpleomorphic (up to 2× variation in size)	Nonpleomorphic (very uniform)
Cytoplasm	Scanty to moderate amount of faintly eosinophilic cytoplasm	Scanty to moderate amount of faintly eosinophilic cytoplasm	Scanty/nondistinct
Mitotic activity	Usually < 5 MF/10 HPF	> 10 MF/10 HPF	< 5 MF/10 HPF
Necrosis	Sometimes	Frequent	Absent

*With the presence of mixed round cell component and spindle cell component.

other primary uterine tumors examined to date contained a high-grade round cell component.

In contrast to *JAZF1*-rearranged ESS, in which tumors are typically positive for ER, PR, and CD10, immunostaining in *YWHAE-FAM22* ESS for ER and PR was focal (< 5%) in the round cell component, and CD10 immunostaining was consistently negative. This suggests that hormonal therapy may be less effective against *YWHAE-FAM22* ESS compared with *JAZF1*-rearranged ESS. Most *YWHAE-FAM22* ESS cases also had a low-grade spindle cell component that morphologically resembled the fibrous variant of ESS and consistently had diffuse ER, PR, and CD10 immunoreactivity but were negative for muscle markers. This profile is similar to what has been reported for the fibrous variant of ESS, in which CD10 immunoreactivity was detected in the fibroblastic component in 3 of 5 tumors, and smooth muscle markers (caldesmon and desmin) were negative.[41] Not surprisingly, the reported immunophenotype for UES has shown variable positivity for these markers as it likely represents a heterogenous population of entities that are not readily classifiable. In fact, the diagnosis of UES should only be considered after exclusion of a poorly differentiated carcinoma, leiomyosarcoma, and carcinosarcoma, all of which may be morphologically similar in appearance. For UES, CD10, ER, and PR, immunoreactivity has been observed in 51% (22/43), 27% (3/11), and 27% (3/11) of tumors examined, respectively.[11,1,17,26,40] It is important to note that the endothelial cells of the stromal capillary network can show weak CD10 immunoreactivity and that many of the ESS cases can contain entrapped myometrial smooth muscle that is immunoreactive for muscle markers; hence, positive staining of these non-neoplastic constituents needs to be excluded when interpreting the immunostaining results.

Among adult mesenchymal and mixed epithelial/mesenchymal tumors, *YWHAE-FAM22* rearrangement is specific for ESS. We recently evaluated the specificity of *YWHAE-FAM22* rearrangement in a series of 40 different adult gynecologic and nongynecologic mesenchymal or mixed epithelial/mesenchymal neoplasms, including uterine leiomyoma, leiomyosarcoma, adenosarcoma, carcinosarcoma, and UES (with nuclear pleomorphism). [23] Aside from ESS, *YWHAE-FAM22* genetic rearrangement was not identified in other adult tumor types examined. Furthermore, *YWHAE* rearrangement and *JAZF1* rearrangement were mutually exclusive.

With regard to tumor nomenclature, we believe that these *YWHAE-FAM22* uterine sarcomas should be categorized as ESS because: (1) all *YWHAE-FAM22* uterine tumors had extensive permeative growth through the myometrium with vascular invasion, similar to that seen in classic low-grade ESS; (2) all *YWHAE-FAM22* ESS also displayed features of established histologic variants of ESS, namely, those with fibromyxoid and sex-cord–like differentiation; and (3) the low-grade spindle cell component exhibited an immunophenotypic characteristic of endometrial stroma, being positive for ER, PR, and CD10, while lacking immunophenotypic evidence for smooth muscle, perivascular epithelioid cell, or epithelial differentiation, whereas the higher-grade component lost expression of these markers. In addition, even though *YWHAE-FAM22* ESS exhibits higher-grade nuclear features compared with *JAZF1*-rearranged ESS, it does not display marked nuclear pleomorphism (< 3 to 1 variation in nuclear size), which distinguishes it from most UESs.

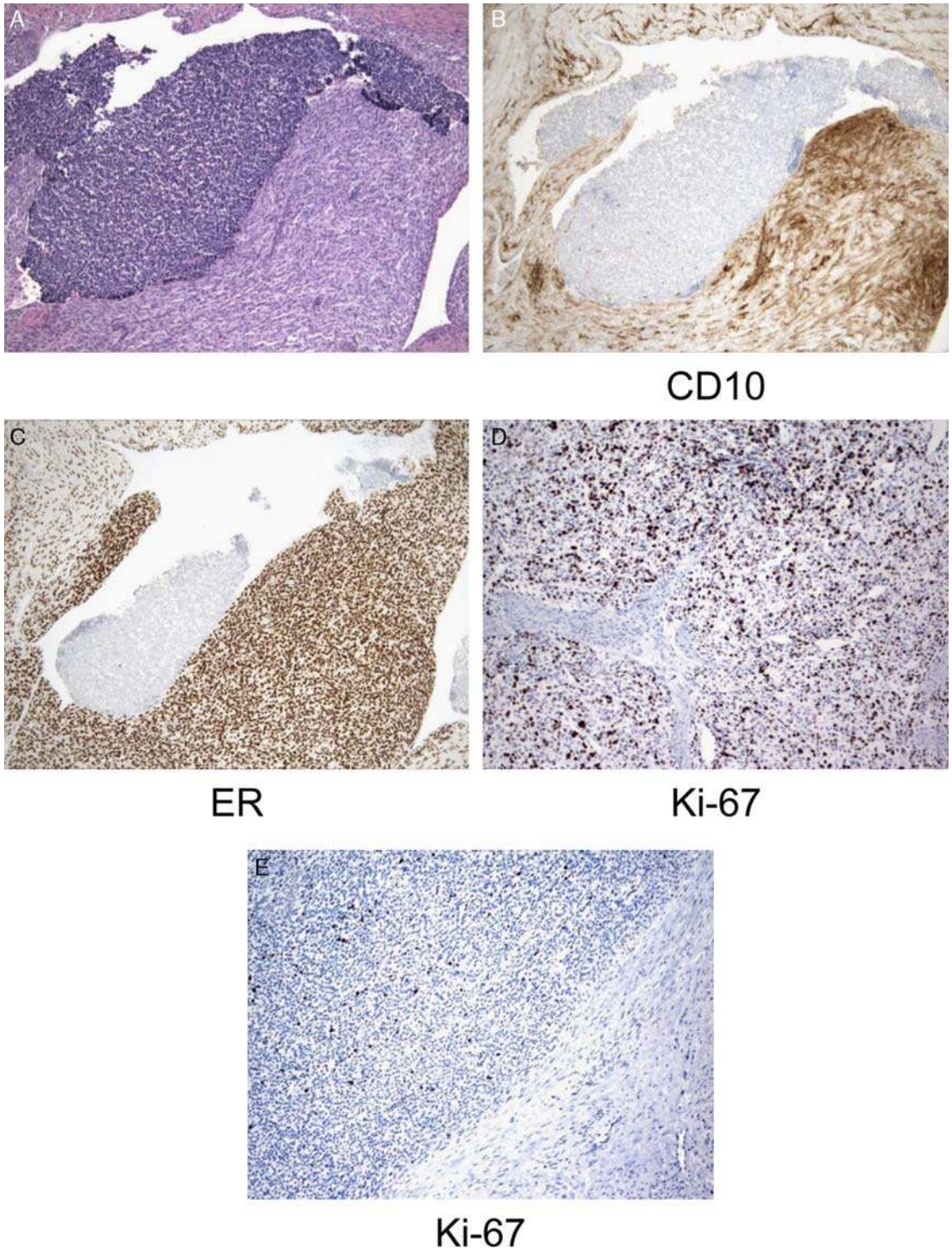

FIGURE 5. Representative images of the CD10 and ER immunostaining pattern in the cellular high-grade round cell component and the low-grade spindle cell component in a *YWHAE-FAM22* ESS (A–C). Representative images of the Ki-67 immunostaining in a *YWHAE-FAM22* ESS (D) and *JAZF1*-rearranged ESS (E).

Importantly, Chang et al[8] have previously described a group of high-grade ESS characterized by nuclei that are uniform with delicate chromatin, but slightly enlarged, with more irregular nuclear membrane than usual low-grade ESS; this is similar to what is shown here for *YWHAE-FAM22* ESS. Furthermore, they observed an

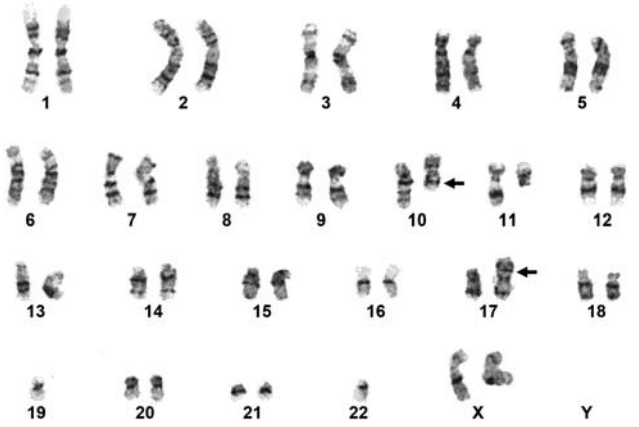

FIGURE 6. Karyotype of *YWHAE-FAM22* ESS (case 3, Table 1) showing t(10;17)(q22;p13) (arrows).

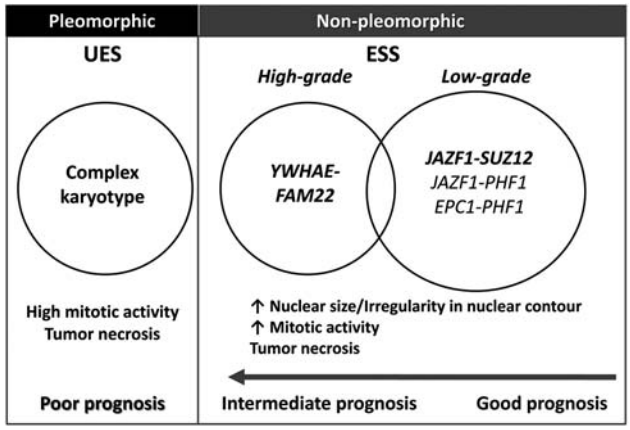

FIGURE 7. Proposed classification for pure uterine sarcomas.

association between high-stage disease and a concomitant increase in both the degree of nuclear atypia and mitotic activity. It is therefore highly probable that at least some of the high-grade ESS cases with high-stage disease described and depicted in their series may be *YWHAE-FAM22* ESS. On that note, we believe that it is reasonable to use the terminology high-grade ESS to describe *YWHAE-FAM22* ESS. However, a genotype-based nomenclature—ESS with *JAZF1* rearrangement and ESS with *YWHAE* (or 14-3-3)-rearrangement—would represent the most biologically accurate disease nomenclature. As for the proposed terminology of undifferentiated endometrial sarcoma with nuclear uniformity (UES-U) proposed by Kurihara et al,[20] a subset of the 7 UES-U cases described in their series may represent *YWHAE-FAM22* ESS; 1 represented a *JAZF1*-rearranged ESS with classic low-grade ESS component and an apparently transformed high-grade component (ie, dedifferentiation). However, there were no differences in disease prognosis/behavior between UES-U and undifferentiated endometrial sarcoma with nuclear pleomorphism (UES-P). In contrast to the UES-P, in which 3 of the 5 patients died of the disease (within 3 y after disease diagnosis), or the UES-U, in which 4 of the 7 patients died of disease (all within 1½ y after disease diagnosis),[20] it is evident that *YWHAE-FAM22* ESS as shown in the current series does not behave in such an aggressive manner. We therefore do not favor the use of UES-U terminology, particularly as the series described was small in size (n = 7) and genetically heterogenous. More importantly, *YWHAE-FAM22* ESS is not truly undifferentiated as it frequently contains a better differentiated low-grade spindle cell component that recapitulates the immunophenotype of endometrial stroma.

We believe that the current evidence indicates that *YWHAE-FAM22* ESS is intermediate between *JAZF1*-rearranged ESS and UES (ie, with nuclear pleomorphism) in terms of malignant potential. We thereby propose a revised classification for uterine sarcomas on the basis of the improved genetic understanding (Fig. 7). An overlap between low-grade ESS and high-grade ESS is indicated in the Venn diagram because *YWHAE-FAM22* can contain a low-grade spindle cell component, which shares morphologic overlap with the low-grade fibrous or fibromyxoid variant of ESS.[33,41] Although it is plausible that some of the previously described fibrous/fibromyxoid ESS cases were *YWHAE-FAM22* ESS, none of these cases were reported to have an accompanying high-grade component, and the mitotic activity was generally low (< 10 MF/10 HPF). It therefore appears likely that at least a subset of the fibrous/fibromyxoid variant of ESS reported is genetically distinct from *YWHAE-FAM22* ESS. Diagnostically, we recommend the use of FISH or RT-PCR studies to confirm the presence of *YWHAE-FAM22* genetic fusion for all nonpleomorphic uterine sarcomas showing either: (1) a biphasic growth pattern with high-grade round cell component and low-grade spindle cell component; (2) purely round cell morphology that is histologically high grade; or (3) purely low-grade spindle cell morphology in a fibrous or fibromyxoid matrix. More importantly, adequate tumor tissue sampling in a resection specimen should be performed, particularly if only low-grade fibrous/fibromyxoid spindle cell morphology is observed.

An intriguing parallel to the t(10;17)(q22;p13)-induced *YWHAE-FAM22* genetic fusion seen in ESS is the identical recurrent translocation reported in clear cell sarcoma of the kidney.[6,35,36] Clear cell sarcoma of the kidney is a rare sarcoma that occurs nearly exclusively in the pediatric age group, virtually all patients being under 5 years of age at presentation. There is a slight male predominance. Although there is no epidemiologic or anatomic overlap between *YWHAE-FAM22* ESS and clear cell sarcoma of the kidney, there is a remarkable histologic resemblance between clear cell sarcoma of the kidney and the round cell component of *YWHAE-FAM22* ESS, particularly in areas where the round tumor cells possess a moderate amount of cytoplasm. Genetically, *YWHAE-FAM22* fusion has been identified recently in the subset of clear cell sarcoma of the kidney with t(10;17).[34] These findings suggest a shared oncogenetic

basis in subsets of ESS and clear cell sarcoma of the kidney and provide another example of fusion oncogene mechanisms with transforming activity in different and distinct disease entities. Other examples of mesenchymal oncogene permissiveness include the *ETV6-NTRK3* genetic fusion seen in both infantile fibrosarcoma and secretory breast cancer[18,39] and the *TPM3-ALK* fusions in inflammatory myofibroblastic tumor and anaplastic large cell lymphoma.[21,22]

In the current study, we provide a detailed description of histologic and immunohistochemical features for *YWHAE-FAM22* ESS. These tumors display high-grade (but nonpleomorphic) round cell histology that is immunophenotypically undifferentiated and frequently includes an admixed low-grade spindle cell component with fibrous/fibromyxoid stroma that is positive for ER, PR, and CD10 immunohistochemically. *YWHAE-FAM22* ESS represents a clinically aggressive subtype of ESS, and its distinction from usual low-grade ESS with *JAZF1* rearrangement is important to guide clinical management.

REFERENCES

1. Abeler VM, Nenodovic M. Diagnostic immunohistochemistry in uterine sarcomas: a study of 397 cases. *Int J Gynecol Pathol*. 2011;30:236–243.
2. Abeler VM, Royne O, Thoresen S, et al. Uterine sarcomas in Norway. A histopathological and prognostic survey of a total population from 1970 to 2000 including 419 patients. *Histopathology*. 2009;54:355–364.
3. Amant F, Tousseyn T, Coenegrachts L, et al. Case report of a poorly differentiated uterine tumour with t(10;17) translocation and neuroectodermal phenotype. *Anticancer Res*. 2011;31:2367–2371.
4. Amant F, Woestenborghs H, Vandenbroucke V, et al. Transition of endometrial stromal sarcoma into high-grade sarcoma. *Gynecol Oncol*. 2006;103:1137–1140.
5. Bartosch C, Exposito MI, Lopes JM. Low-grade endometrial stromal sarcoma and undifferentiated endometrial sarcoma: a comparative analysis emphasizing the importance of distinguishing between these two groups. *Int J Surg Pathol*. 2010;18:286–291.
6. Brownlee NA, Perkins LA, Stewart W, et al. Recurring translocation (10;17) and deletion (14q) in clear cell sarcoma of the kidney. *Arch Pathol Lab Med*. 2007;131:446–451.
7. Chan JK, Kawar NM, Shin JY, et al. Endometrial stromal sarcoma: a population-based analysis. *Br J Cancer*. 2008;99:1210–1215.
8. Chang KL, Crabtree GS, Lim-Tan SK, et al. Primary uterine endometrial stromal neoplasms. A clinicopathologic study of 117 cases. *Am J Surg Pathol*. 1990;14:415–438.
9. Chew I, Oliva E. Endometrial stromal sarcomas: a review of potential prognostic factors. *Adv Anat Pathol*. 2010;17:113–121.
10. Chiang S, Ali R, Melnyk N, et al. Frequency of known gene rearrangements in endometrial stromal tumors. *Am J Surg Pathol*. 2011;35:1364–1372.
11. D'Angelo E, Spagnoli LG, Prat J. Comparative clinicopathologic and immunohistochemical analysis of uterine sarcomas diagnosed using the World Health Organization classification system. *Hum Pathol*. 2009;40:1571–1585.
12. Denschlag D, Masoud I, Stanimir G, et al. Prognostic factors and outcome in women with uterine sarcoma. *Eur J Surg Oncol*. 2007;33:91–95.
13. Garg G, Shah JP, Toy EP, et al. Stage IA vs. IB endometrial stromal sarcoma: does the new staging system predict survival? *Gynecol Oncol*. 2010;118:8–13.
14. Hendrickson MR, Tavassoli FA, Kempson RL. Mesenchymal tumours and related lesions. In: Tavassoli FA, Devilee P. eds. *World Health Organization Classification of Tumours Pathology and Genetics of Tumours of the Breast and Female Genital Organ*. Lyon, France: IARC Press; 2003:233–236.
15. Hrzenjak A, Moinfar F, Tavassoli FA, et al. JAZF1/JJAZ1 gene fusion in endometrial stromal sarcomas: molecular analysis by reverse transcriptase-polymerase chain reaction optimized for paraffin-embedded tissue. *J Mol Diagn*. 2005;7:388–395.
16. Huang HY, Ladanyi M, Soslow RA. Molecular detection of JAZF1-JJAZ1 gene fusion in endometrial stromal neoplasms with classic and variant histology: evidence for genetic heterogeneity. *Am J Surg Pathol*. 2004;28:224–232.
17. Jung CK, Jung JH, Lee A, et al. Diagnostic use of nuclear beta-catenin expression for the assessment of endometrial stromal tumors. *Mod Pathol*. 2008;21:756–763.
18. Knezevich SR, McFadden DE, Tao W, et al. A novel ETV6-NTRK3 gene fusion in congenital fibrosarcoma. *Nat Genet*. 1998;18:184–187.
19. Koontz JI, Soreng AL, Nucci M, et al. Frequent fusion of the JAZF1 and JJAZ1 genes in endometrial stromal tumors. *Proc Natl Acad Sci USA*. 2001;98:6348–6353.
20. Kurihara S, Oda Y, Ohishi Y, et al. Endometrial stromal sarcomas and related high-grade sarcomas: immunohistochemical and molecular genetic study of 31 cases. *Am J Surg Pathol*. 2008;32:1228–1238.
21. Lamant L, Dastugue N, Pulford K, et al. A new fusion gene TPM3-ALK in anaplastic large cell lymphoma created by a (1;2)(q25;p23) translocation. *Blood*. 1999;93:3088–3095.
22. Lawrence B, Perez-Atayde A, Hibbard MK, et al. TPM3-ALK and TPM4-ALK oncogenes in inflammatory myofibroblastic tumors. *Am J Pathol*. 2000;157:377–384.
23. Lee CH, Ou WB, Mariño-Enriquez A, et al. 14-3-3 fusion oncogene in high-grade endometrial stromal sarcoma. *Proc Natl Acad Sci USA*. 2012;109:929-934.
24. Leunen K, Amant F, Debiec-Rychter M, et al. Endometrial stromal sarcoma presenting as postpartum haemorrhage: report of a case with a sole t(10;17)(q22;p13) translocation. *Gynecol Oncol*. 2003;91:265–271.
25. Liegl B, Kepten I, Le C, et al. Heterogeneity of kinase inhibitor resistance mechanisms in GIST. *J Pathol*. 2008;216:64–74.
26. McCluggage WG, Sumathi VP, Maxwell P. CD10 is a sensitive and diagnostically useful immunohistochemical marker of normal endometrial stroma and of endometrial stromal neoplasms. *Histopathology*. 2001;39:273–278.
27. Micci F, Panagopoulos I, Bjerkehagen B, et al. Consistent rearrangement of chromosomal band 6p21 with generation of fusion genes JAZF1/PHF1 and EPC1/PHF1 in endometrial stromal sarcoma. *Cancer Res*. 2006;66:107–112.
28. Micci F, Walter CU, Teixeira MR, et al. Cytogenetic and molecular genetic analyses of endometrial stromal sarcoma: nonrandom involvement of chromosome arms 6p and 7p and confirmation of JAZF1/JJAZ1 gene fusion in t(7;17). *Cancer Genet Cytogenet*. 2003;144:119–124.
29. Nucci MR, Harburger D, Koontz J, et al. Molecular analysis of the JAZF1-JJAZ1 gene fusion by RT-PCR and fluorescence in situ hybridization in endometrial stromal neoplasms. *Am J Surg Pathol*. 2007;31:65–70.
30. Ohta Y, Suzuki T, Omatsu M, et al. Transition from low-grade endometrial stromal sarcoma to high-grade endometrial stromal sarcoma. *Int J Gynecol Pathol*. 2010;29:374–377.
31. Oliva E, Clement PB, Young RH. Endometrial stromal tumors: an update on a group of tumors with a protean phenotype. *Adv Anat Pathol*. 2000;7:257–281.
32. Oliva E, de Leval L, Soslow RA, et al. High frequency of JAZF1-JJAZ1 gene fusion in endometrial stromal tumors with smooth muscle differentiation by interphase FISH detection. *Am J Surg Pathol*. 2007;31:1277–1284.
33. Oliva E, Young RH, Clement PB, et al. Myxoid and fibrous endometrial stromal tumors of the uterus: a report of 10 cases. *Int J Gynecol Pathol*. 1999;18:310–319.
34. O'Meara E, Stack D, Lee CH, et al. Characterisation of the chromosomal translocation t(10;17)(q22;p13) in clear cell sarcoma

of kidney. *J Pathol*. 2012. doi: 10.1002/path.3985. [Epub ahead of print].
35. Punnett HH, Halligan GE, Zaeri N, et al. Translocation 10;17 in clear cell sarcoma of the kidney. A first report. *Cancer Genet Cytogenet*. 1989;41:123–128.
36. Rakheja D, Weinberg AG, Tomlinson GE, et al. Translocation (10;17)(q22;p13): a recurring translocation in clear cell sarcoma of kidney. *Cancer Genet Cytogenet*. 2004;154:175–179.
37. Regauer S, Emberger W, Reich O, et al. Cytogenetic analyses of two new cases of endometrial stromal sarcoma—non-random reciprocal translocation t(10;17)(q22;p13) correlates with fibrous ESS. *Histopathology*. 2008;52:780–783.
38. Sandberg AA. The cytogenetics and molecular biology of endometrial stromal sarcoma. *Cytogenet Genome Res*. 2007;118:182–189.
39. Tognon C, Knezevich SR, Auntsman D, et al. Expression of the ETV6-NTRK3 gene fusion as a primary event in human secretory breast carcinoma. *Cancer Cell*. 2002;2:367–376.
40. Vera AA, Guadarrama MB. Endometrial stromal sarcoma: clinicopathological and immunophenotype study of 18 cases. *Ann Diagn Pathol*. 2011;15:312–317.
41. Yilmaz A, Rush DS, Soslow RA. Endometrial stromal sarcomas with unusual histologic features: a report of 24 primary and metastatic tumors emphasizing fibroblastic and smooth muscle differentiation. *Am J Surg Pathol*. 2002;26:1142–1150.